A hybrid control method to suppress the three times fundamental frequency neutral-point voltage fluctuation in a VIENNA rectifier

***Abstract*—This paper presents a solution to the control of the three times fundamental frequency fluctuation of the neutral-point in a VIENNA rectifier. A hybrid method combining a dynamic adjustment factor with a voltage deviation control of the split DC-link is proposed. The fluctuation of the neutral-point has been analyzed and the reason for the three times fundamental frequency fluctuation has been described using a mathematic model. As well as minimizing the three times fundamental frequency component in the neutral-point voltage the proposed control method also provides immunity to the influence of changes in the capacitor voltage. Furthermore, significant fluctuation in the neutral-point voltage caused by asymmetric capacitor parameters or unbalanced load can be effectively reduced by using a hybrid control method combining additional adjustment coefficients. The feasibility and effectiveness of the proposed strategy has been verified through the presented simulation and experimental results.**

***Index Terms*—VIENNA rectifier; neutral-point fluctuation; hybrid control method; dynamic adjustment factor**

I. INTRODUCTION

A grid-connected voltage source pulse width modulated(PWM) rectifier has advantages over a diode bridge rectifier in terms of having a low current total harmonic distortion (THD) as well as offering controllable supply side power factor (PF) [1]-[3]. In comparison to the traditional two and three-level unidirectional PWM rectifiers [4]-[5], the VIENNA rectifier is reported to have the advantages of: a simple power stage structure and control; low input current harmonics and low device voltage stress [6] -[9]. Therefore, they are widely used in telecommunications power systems, aircraft and medium-voltage drive systems, where high-power density and low device voltage stresses are required [10]–[12].

The VIENNA rectifier belongs to the three-level voltage source converter family [13]–[14]. This three-level structure results in a low blocking voltage stress on the power semiconductor devices and a small input inductor volume. However, it can also cause a significant problem related to the fluctuation of the neutral-point voltage, which can cause unbalanced capacitor voltages leading to

increased stress on semiconductor devices and the generation of low-order harmonics in the input voltages and currents [15] –[16]. A series of suppression methods for neutral-point fluctuation in the VIENNA rectifier have been proposed [17]–[21], these methods can be classified into the following categories:

- Solutions based on the use of P and N short vectors[17] or redundant switching states[18];
- Solutions based on the injection of zero-sequence or ripple components[18] ,[19];
- Solutions with neutral-point voltage error feed-forward [20]–[22] where any deviation of the voltage across the two DC link capacitors is added to the modulation waveform to suppress the neutral-point offset.

In [17], a hysteresis-band based method to eliminate the potential effect on the neutral-point according to the principle that the P and N short vectors have the opposite effect on neutral-point voltage. However, this method relies on a complicated three-level modulation strategy. In [18], the output voltage neutral-point was balanced by using a proper distribution of the local overall on-time of the redundant switching during each half period. The input current however would be influenced in a negative way for an asymmetric output load because of the change in the distribution of the switching states [18] resulting in increased low order harmonics. Wang et al [18] used injected zero-sequence components to suppress the neutral-point fluctuation, but the calculation of the zero-sequence components is very complex and difficult to realize in practice. A constant power control by injecting power ripple was employed to eliminate the twice fundamental frequency ripple in the DC-link voltage in [20], however, it does not consider the three times fundamental frequency fluctuation. Reference [21] describes a zero-sequence component injected carrier-based SPWM with the equivalent voltage transfer ratio and voltage utilization ratio of SVPWM. This method avoided using the complex three-level SVPWM strategy, but a large calculation effort is required for the zero-sequence components. A feed-forward control method with neutral-point voltage error was used to improve neutral-point performance through employing a fixed regulating factor in [22], however, the selection of regulating factor lacks theoretical basis and only depends on engineering experience, furthermore, this scheme has some difficulty in reducing the three times fundamental frequency fluctuation. Reference [22] proposed two further methods named active and passive voltage-balancing technology to balance the DC-link capacitor voltages for a multi-pulse rectifier.

This paper presents a hybrid method combining a dynamic adjustment factor with a capacitance voltage deviation expression to suppress the three times fundamental frequency neutral-point voltage fluctuations for the VIENNA rectifier. The feasibility and effectiveness of the proposed strategy has been verified through simulation and experimental results.

II. Neutral-point Mathematical Model in a VIENNA Rectifier

Fig. 1 shows the circuit topology of the non-regenerative three-level VIENNA rectifier considered in this paper. The circuit is

comprised of a main diode bridge and three bidirectional switches connecting the input phases to the DC-link neutral-point. The three active switching units are controlled to ensure sinusoidal input current and a steady DC-link voltage.

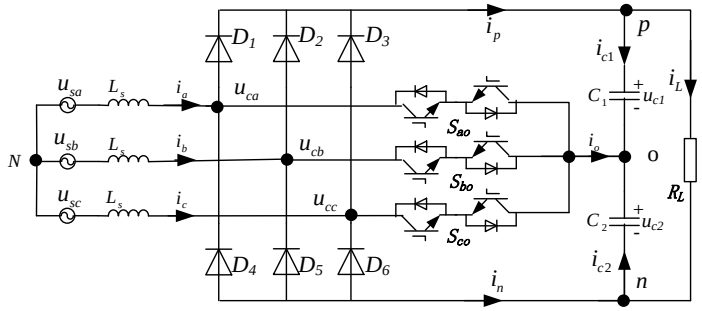

Fig. 1. Topology of VIENNA rectifier

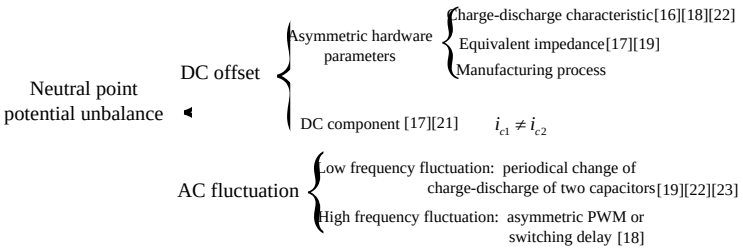

Fig. 2. The neutral-point potential unbalanced forms

A. Reason of Neutral-point Voltage Unbalance

By analyzing the VIENNA rectifier circuit as shown in Fig.1, the relationship expression between voltage and current for the DC-link capacitors can be described as

$$\begin{aligned} i_{c1} &= C_1 \frac{du_{c1}}{dt} \\ i_{c2} &= -C_2 \frac{du_{c2}}{dt} \end{aligned} \tag{1}$$

By integrating equation (1), the voltage of each capacitor can be written as follows:

$$\begin{aligned} \int_0^t i_{c1} dt = C_1 u_{c1}(t) - C_1 u_{c1}(0) \quad &\Rightarrow \quad u_{c1}(t) = \frac{1}{C_1}\int_0^t i_{c1} dt + u_{c1}(0) \\ \int_0^t i_{c2} dt = -C_2 u_{c2}(t) + C_2 u_{c2}(0) \quad &\Rightarrow \quad u_{c2}(t) = -\frac{1}{C_2}\int_0^t i_{c2} dt + u_{c2}(0) \end{aligned} \tag{2}$$

Where i_{c1},i_{c2} and $u_{c1}(t)$, $u_{c2}(t)$ are the charge-discharge currents and voltages of DC-link capacitors of c1 and c2 respectively,$u_{c1}(0)$and $u_{c2}(0)$ are the initial voltage of the two capacitors.

Seen from equation (2), the voltage of the capacitors is not only related to the initial capacitor voltage value, but also to the charge-discharge currents in real time. The different manufacturing processes or stray parameters of capacitor can cause different charge-discharge characteristics and equivalent impedances, which finally result in the form of capacitor voltage unbalance. In this operating situation, the neutral-point current contains large amounts of AC fluctuation and DC offset components causing neutral-point voltage unbalance [24]. Based on analyzing a large amount of references on developments and reports into neutral-point unbalance, the neutral-point potential unbalanced forms and reasons can be categorized in Fig.2 [17-20] [22-24].

From Eqn.2, the neutral-point potential unbalance becomes present since the charge-discharge currents of the two capacitors is not equal on average to zero, while neutral-point fluctuation is only the expression form of the charge-discharge current flow

through the capacitors .

Therefore, it is necessary to develop mathematical model for the neutral-point current to study the changing trend of neutral-point charge-discharge currents so that an effective method to suppress neutral-point fluctuation can be found.

B. Neutral-point Current Mathematical Model

In order to simplify the analysis, the following assumptions have been made:

1) DC-link output voltage is regarded as ideal DC voltage source;

2) Input voltage and modulation signal are three phase balanced;

3) Power switches and lines are regarded as ideal components.

As shown in Fig.1, current equations of node p,o and n can be derived according to the Kirchhoff's current law as follows:

$$\begin{cases} i_p = i_{c1} + i_L \\ i_{c1} = C_1 \dfrac{du_{c1}}{dt} \end{cases} \tag{3}$$

$$\begin{cases} i_n = i_{c2} - i_L \\ i_{c2} = -C_2 \dfrac{du_{c2}}{dt} \end{cases} \tag{4}$$

$$\begin{cases} i_o = -(i_{c1} + i_{c2}) = C_2 \dfrac{du_{c2}}{dt} - C_1 \dfrac{du_{c1}}{dt} \\ i_o = s_{ao} i_a + s_{bo} i_b + s_{co} i_c \end{cases} \tag{5}$$

S_{jo} represents the switching functions and can be defined as:

$$s_{jo} = \begin{cases} 0 & \text{S}_{\text{jo}} \text{ on} \\ 1 & \text{S}_{\text{jo}} \text{ off and } u_{\text{sj}} > 0 \\ -1 & \text{S}_{\text{jo}} \text{ off and } u_{\text{sj}} < 0 \end{cases} \quad j=\text{a,b,c} \tag{6}$$

To simplify the analysis, the initial voltage of capacitor is ignored, so, $u_{c1} = u_{c1}(t)$, $u_{c2} = u_{c2}(t)$, and by integrating from equation (5), we have

$$C_2 u_{c2} - C_1 u_{c1} = \int_0^t i_o dt = \int_0^t \left(s_{ao} i_a + s_{bo} i_b + s_{co} i_c \right) dt \tag{7}$$

Seen from equation (7), the reason for neutral-point potential voltage fluctuation is caused by the non-zero neutral-point current derived from the high frequency charge-discharge of DC-link capacitors.

C. The Three Times Fundamental Frequency Fluctuation of Neutral-point Current

In order to simplify the analysis, the value of C_1 is set to be equal to C_2, using the fundamental functions of high frequency switch instead of high frequency switching functions in the equation (5), so the fundamental model of neutral-point current can be obtained as:

$$\begin{cases} i_o = (\dfrac{du_{c2}}{dt} - \dfrac{du_{c1}}{dt})C \\ i_o = (1-|u_{ma}|)i_a + (1-|u_{mb}|)i_b + (1-|u_{mc}|)i_c \end{cases} \tag{8}$$

Where u_{ma},u_{mb} and u_{mc} are the three phase input voltage reference signals which are in phase with three phase grid-side voltages, respectively

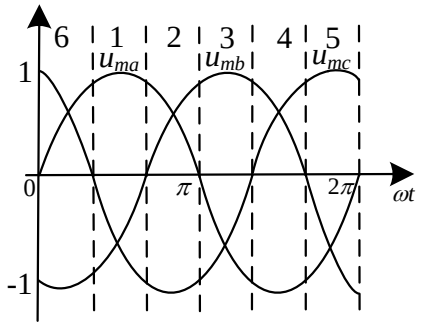

Fig. 3. Sector definition of VIENNA rectifier

In order to find out how the neutral-point current changes in one period and to obtain a mathematical model for the neutral-point current in every sector. The three-phase input sinusoidal voltage reference signals are divided into six intervals (sectors) as shown in Fig.3. In each interval, the absolute value of one phase voltage reference signal is maximum, the other two phase reference signals are opposite polarity over this phase. For example, in interval 1, u_{ma} is more than zero and its absolute value is maximum, u_{mb} and u_{mc} are less than zero, so it can be written as follows

$$u_{ma} > 0, u_{mb} < 0, u_{mc} < 0 \tag{9}$$

Similarly, an expression of all other intervals also can be obtained.

Substituting (9) into (8), we can achieve the expression of the fundamental frequency neutral-point current, which is given by:

$$i_o = (1-u_{ma})i_a + (1+u_{mb})i_b + (1+u_{mc})i_c \tag{10}$$

Meanwhile, the sum of all the phase currents is zero in a three-phase symmetric system, then (10) can be simplified as:

$$i_o = -u_{ma}i_a + u_{mb}i_b + u_{mc}i_c \tag{11}$$

In addition, for the three-phase three-wire system it follows that:

$$u_{ma} + u_{mb} + u_{mc} = 0 \tag{12}$$

When the input current is in phase with grid side voltage in a steady state system with a closed-loop control, the instantaneous phase current can be described as [22]:

$$i_j = k \cdot u_{mj},\ j = a, b, c \qquad (13)$$

Where k is the ratio coefficient between the current and reference voltage amplitude, which is a constant positive value. j indicates the three-phase input, which can be a, b or c.

With (11), (12) and (13), the neutral-point fundamental frequency current is given by:

$$i_o = -2k u_{mb} u_{mc} \qquad (14)$$

In sector 1, u_{mb} and u_{mc} have the same polarity, so it follows that:

$$i_o < 0 \qquad (15)$$

Equation (15) shows that the fundamental frequency component of the neutral-point current is less than zero in sector.1, where the DC-link capacitor C_1 charges and C_2 discharges, furthermore, the voltage of capacitor C_1(U_{c1}) is greater than the voltage of capacitor C_2(U_{c2}).

The expressions of neutral-point current and relationship between two capacitors in the other five sectors can be obtained as listed in Tab. I in the same way. Seen from Tab. I, the neutral-point current can be expressed as the product of two sinusoidal signals, which only equal zero at the beginning and end of the sector and change with a sinusoidal tendency in real time, the neutral-point low frequency voltage fluctuation becomes present since these low frequency distortion signals of neutral-point current are not always equal to zero.

TABLE I

NEUTRAL-POINT CURRENT EXPRESSIONS AND ITS EFFECT IN EACH SECTOR

Sector	Neutral-point current expressions	Charge and discharge of two capacitors or Voltage relationship between two capacitors
1	$i_o=-2ku_{mb}u_{mc}<0$	charge C_1, discharge C_2, $U_{c1}>U_{c2}$
2	$i_o=2ku_{mb}u_{ma}>0$	dischargeC_1,chargeC_2, $U_{c1}<U_{c2}$
3	$i_o=-2ku_{ma}u_{mc}<0$	chargeC_1,dischargeC_2, $U_{c1}>U_{c2}$
4	$i_o=2ku_{mb}u_{mc}>0$	dischargeC_1,chargeC_2, $U_{c1}<U_{c2}$
5	$i_o=-2ku_{mb}u_{ma}<0$	chargeC_1,dischargeC_2, $U_{c1}>U_{c2}$
6	$i_o=2ku_{ma}u_{mc}>0$	dischargeC_1,chargeC_2, $U_{c1}<U_{c2}$

A

IS

$$\Delta_{uc} = U_{c2} - U_{c1} \qquad (16)$$

Reference [22] used a method based on this neutral point voltage deviation with a fixed adjustment factor to compensate the

neutral point voltage fluctuation, however, this conventional fixed adjustment factor method has some difficulty in reducing the low frequency neutral point fluctuations.

The low frequency neutral point fluctuation would be eliminated if this neutral-point voltage deviation could be adjusted by using an appropriate dynamic adjustment factor [22]. For this reason a method with a dynamic adjustment factor is deduced as follows:

In the first sector as shown in Fig.3, substituting the neutral-point voltage offset with adjustment coefficient m_d as a compensation component into (10), the neutral-point current can be described as follows:

$$i_o' = (1-u_{ma}-m_d\Delta_{uc})i_a + (1+u_{mb}+m_d\Delta_{uc})i_b + (1+u_{mc}+m_d\Delta_{uc})i_c \qquad (17)$$

With (10), (12) and (13), then (17) can be simplified as

$$i_o' = i_o - 2m_d k u_{ma}\Delta_{uc} \qquad (18)$$

With the introduction of neutral-point deviation, a further part can be added to the neutral-point current fundamental expression reducing neutral-point current amplitude and restraining the neutral-point voltage offset.

From the analysis in section II, the neutral-point voltage fluctuation becomes present where the fundamental frequency components of the neutral-point current are not equal to zero. Therefore, if (18) is equal zero, then the neutral-point current fundamental frequency components are always constant and zero, thus the neutral-point offset could be theoretically eliminated and the neutral-point fluctuation would be removed, combing (14), we have:

$$m_d = -\frac{u_{mb}u_{mc}}{u_{ma}\Delta_{uc}} \qquad (19)$$

Where m_d is the dynamic adjustment factor for neutral-point. From this equation, the dynamic adjustment expression can be resolved, and its expression can be deduced as follows:

$$u_{md} = m_d\Delta_{uc} = -\frac{u_{mb}u_{mc}}{u_{ma}} \qquad (20)$$

The neutral-point dynamic adjustment factors and expression in other sectors can be similarly obtained as shown in Tab. II, which shows the influence on the fundamental frequency component and three times fundamental frequency component are all shown in this table.

TABLE II
DYNAMIC ADJUSTMENT FACTOR AND EXPRESSION

Sector	Dynamic adjustment factor m_d	Dynamic adjustment expression u_{md}	influence to fundamental frequency component	influence to three times frequency fluctuation
1,4	$m_d = -\frac{u_{mb}u_{mc}}{u_{ma}\Delta_{uc}}$	$u_{md} = -\frac{u_{mb}u_{mc}}{u_{ma}}$	reduced	reduced
2,5	$m_d = -\frac{u_{mb}u_{ma}}{u_{mc}\Delta_{uc}}$	$u_{md} = -\frac{u_{mb}u_{ma}}{u_{mc}}$	reduced	reduced
3,6	$m_d = -\frac{u_{ma}u_{mc}}{u_{mb}\Delta_{uc}}$	$u_{md} = -\frac{u_{ma}u_{mc}}{u_{mb}}$	reduced	reduced

B. HYBRID METHOD TO SUPPRESS NEUTRAL-POINT FLUTUATION COMBINING A DYNAMIC ADJUSTMENT FACTOR AND CAPACITOR VOLTAGE DEVIATION

Equation (19) is a theoretical condition to eliminate the offset of neutral-point, which requires that the value of the dynamic adjustment factor is close to infinite as shown in the following, but that is impossible to achieve, in other words, the value of the dynamic adjustment factor method is decided by the deviation of neutral point itself in order to suppress neutral-point fluctuations. So this method can not eliminate but only decrease the neutral-point potential fluctuation. To achieve a better performance for neutral point control, a hybrid method combining a dynamic adjustment factor with capacitor voltage deviation is proposed and deduced as follows.

$$\lim_{\Delta_{uc}\to 0}(m_d = -\frac{u_{mb}u_{mc}}{u_{ma}\Delta_{uc}}) = +\infty \qquad (21)$$

The hybrid neutral point control method consists of two parts: the actual neutral-point deviation u_{m0} and the dynamic adjustment expression u_{md} including the dynamic adjustment factor， then the hybrid adjustment expression u_{m} can be expressed as follows:

$$u_m = u_{m0} + u_{md} \qquad (22)$$

In the first sector as shown in Fig.3, the dynamic adjustment expression is shown in equation (20). If not considering the influence of asymmetric capacitance parameters or unbalanced load, u_{m0} can be written as:

$$u_{m0} = \Delta_{uc} = U_{c2} - U_{c1} \qquad (23)$$

Where u_{m0} is the voltage deviation of DC-link two capacitors.

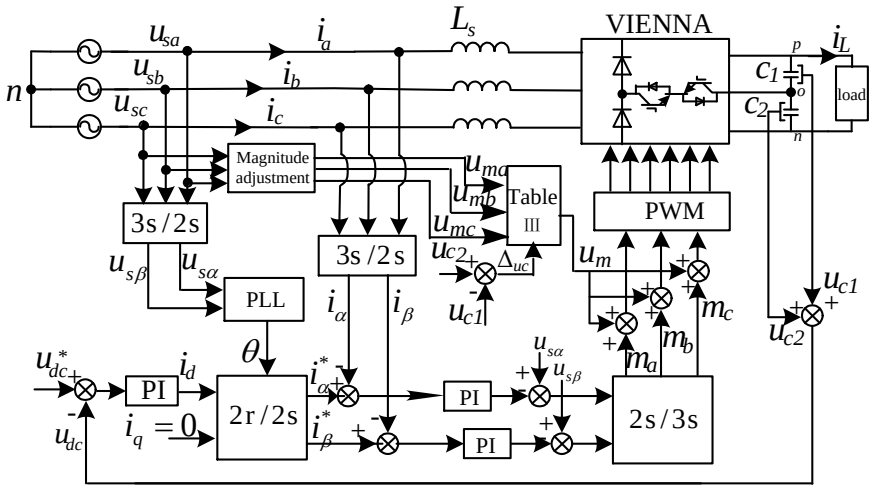

Fig.4 The dual closed loop control system block diagram based on hybrid neutral-point control method

Similarly, expressing in equation (20), the hybrid adjustment factor m can be developed as

$$m = 1 - \frac{u_{mb}u_{mc}}{u_{ma}\Delta_{uc}} \qquad (25)$$

The neutral-point hybrid adjustment factor and adjustment expression in remaining sectors can be similarly obtained as shown in

Table. III. The dual closed loop control system based on hybrid neutral-point suppression method in a VIENNA rectifier is shown in Fig.4. Through the above analysis and Fig.4, it can be seen that the neutral point fluctuation of VIENNA rectifier would be effectively eliminated using proposed hybrid neutral point control method combining the capacitor voltage deviation with dynamic adjustment factor based on a closed loop control. Moreover, seen from Table. III , the neutral point fluctuation control only needs a simple look up table instead of the need for any complex computations, which renders this method very suitable for implementation in a real controller.

TABLE III
HYBRID ADJUSTMENT FACTORS AND EXPRESSIONS

Sector	Hybrid adjustment factor $m=m_0+m_d$	Hybrid adjustment expression $u_m=u_{m0}+u_{md}$
1,4	$m=1-\frac{u_{mb}u_{mc}}{u_{ma}\Delta_{uc}}$	$u_m=\Delta_{uc}-\frac{u_{mb}u_{mc}}{u_{ma}}$
2,5	$m=1-\frac{u_{mb}u_{ma}}{u_{mc}\Delta_{uc}}$	$u_m=\Delta_{uc}-\frac{u_{mb}u_{ma}}{u_{mc}}$
3,6	$m=1-\frac{u_{mc}u_{ma}}{u_{mb}\Delta_{uc}}$	$u_m=\Delta_{uc}-\frac{u_{mc}u_{ma}}{u_{mb}}$

pa tor in order to reduce the influence caused by the abnormal condition, and then the following equation can be obtained:

$$u'_{m0}=k_1\Delta_{uc} \qquad (26)$$

Substituting (26) into (24)-(25), the improved hybrid adjustment factor and expression to reduce the neutral-point fluctuation for this abnormal condition in sector 1 are shown in equation (27) and (28), the equations in other sectors can be obtained similarly and omitted here because of limited length for the paper.

$$m'=k_1-\frac{u_{mb}u_{mc}}{u_{ma}\Delta_{uc}} \qquad (27)$$

$$u'_m=\Delta_{uc}(k_1-\frac{u_{mb}u_{mc}}{u_{ma}\Delta_{uc}}) \qquad (28)$$

C. IDEAL WAVEFORMS ANALYSIS FOR NEUTRAL-POINT FLUTUATION SUPPRESSION METHOD

The equivalent circuit of single-phase VIENNA rectifier is shown in Fig.5 [8]. Seen from Fig.5, the VIENNA rectifier features a boost characteristic as mentioned in reference [26], Reference [27] presents an equivalent circuit model for the boost topology using dependent current and voltage sources as shown in Fig.6. Seen from Fig.1, when the switch is on, the inductor is charged supplied by the power supply, then this operating state can be regarded as a current source [27], when the switch is off, the DC-link capacitors would be charged through the uncontrollable rectifier bridge supplied by the power supply, then its equivalent is a voltage source. Meanwhile the three phase VIENNA rectifier is comprised of three single-phase VIENNA rectifiers in a parallel output [1] [21], hence, the equivalent circuit of three phase VIENNA rectifier also consists of the equivalent model of three single phase

VIENNA rectifiers in parallel as shown in Fig 7. Seen from Fig.7, the neutral point current is controlled by the current source using a switch meanwhile the capacitor voltage is decided by the voltage source.

Combining Fig.1 with the table I, the ideal waveform of neutral-point current i_o can be drawn as shown in Fig.8, the neutral-point current presents a three times fundamental fluctuation. Since the neutral-point current is phase-shifted by 90^0 to the deviation of the two DC-link capacitors because of the capacitor characteristics, then the capacitor voltage deviation can be obtained as shown in the third waveform of Fig.8. According to table II, the waveform of dynamic adjustment expression u_{md} is also shown in Fig.8, presenting a AC signal with the same frequency and phase with i_o, u_{md} is added to the modulated signal and used to generate the PWM waveform u_{rmd} as shown in Fig.8. Seen from Fig.8, the u_{rmd} pulse width is inversely proportion to the i_o magnitude, then this results in a compensation for the neutral-point current fluctuation. Similarly, according to table III, the hybrid expression u_m is drawn in the sixth waveform as well as its corresponding PWM is shown in the seventh waveform in Fig.8. Fig.8 also shows the pulse width of u_{rm} is inversely proportion to the magnitude of u_m consisting of a voltage deviation with a dynamic adjust expression, thus, the fluctuation of capacitor voltage deviation and neutral-point current can all be compensated by using this PWM generated by u_m.

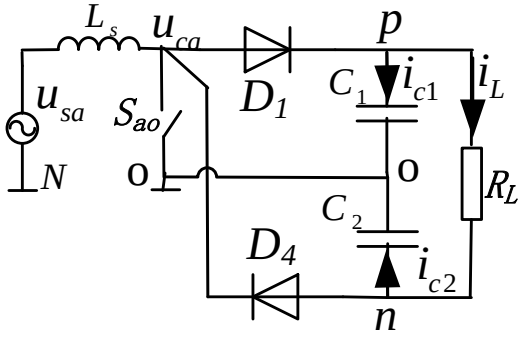

Fig.5 The equivalent circuit of phase a for VIENNA rectifier

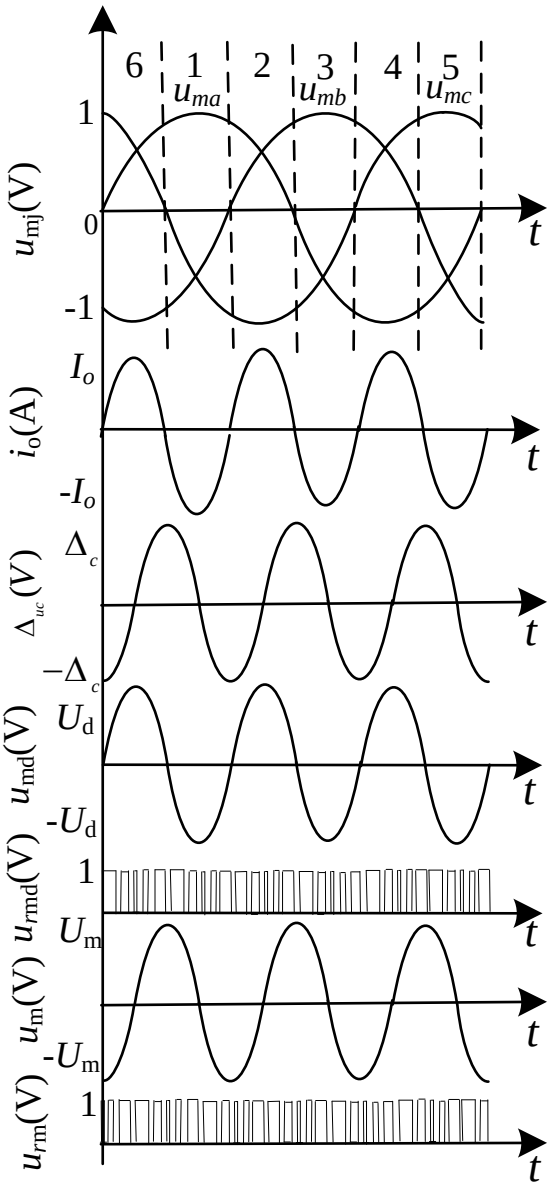

Fig.8 The ideal waveforms of neutral point current, capacitor voltage deviation and adjustment expression

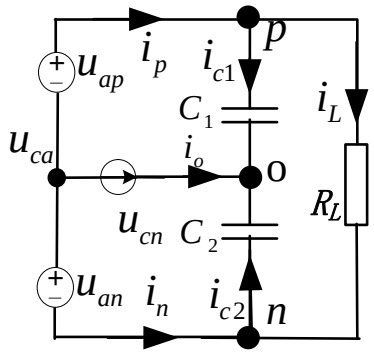

Fig.6 The equivalent circuit of three phase VIENNA rectifier

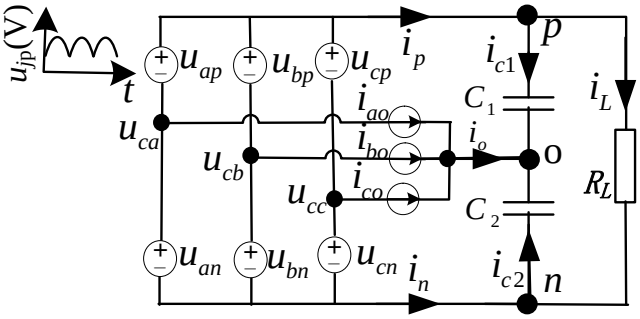

Fig.7 The equivalent circuit of three phase VIENNA rectifier

TABLE IV SYSTEM PARAMETERS

parameter	value
Grid-voltage	100V/50Hz
DC-link voltage reference	200V
Load resistor	800-120Ω
Switching frequency	4.8kHz
AC filter inductor	8mH
DC-link filter capacitor	1600 μF

IV. EXPERIMENT RESULTS

A power converter prototype was built to verify the validation of the proposed neutral-point balance control strategy, which is shown in Fig.9, the closed loop control and hybrid neutral-point control method combining a dynamic adjustment factor with capacitor voltage deviation expression were all carried out using a 32-bit DSP type TMS320F2812 operating at a clock frequency of 150MHz, the experimental parameters are shown in Table IV. The VIENNA rectifier belongs to the three-level voltage source converter family, one of control objectives for multi-level converter is to achieve the low current THD with a low switching frequency, further reducing switching losses, which is the reason of using a low switching frequency shown in table IV.

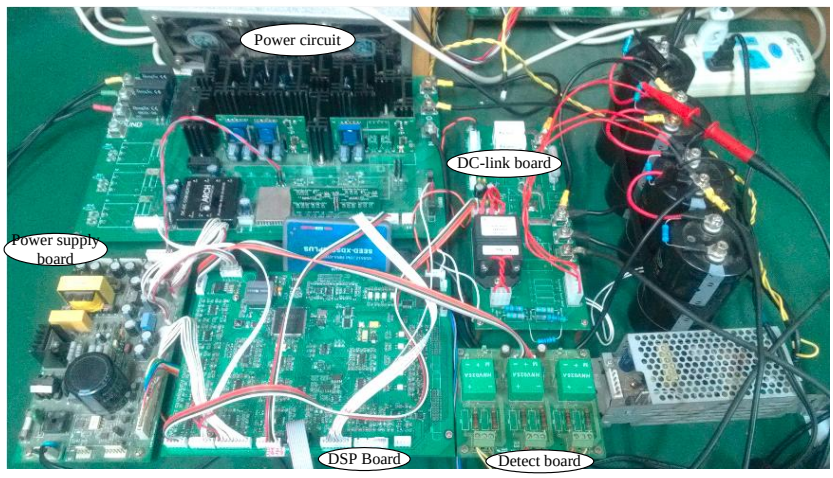

Fig.9 Experimental prototype

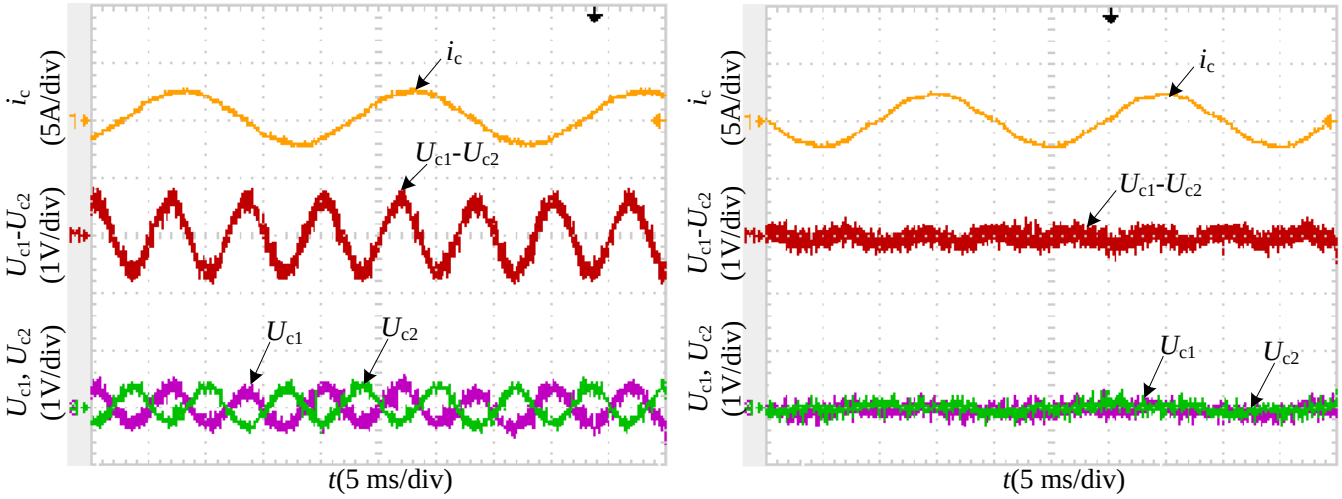

(a) Conventional method (b) Hybrid method

Fig.10 The comparison waveforms between conventional fixed factor and hybrid method

voltage fluctuation is also effectively reduced, which verifies the validity of proposed scheme.

A. Abnormal operating condition (asymmetric capacitor parameter and unbalanced load)

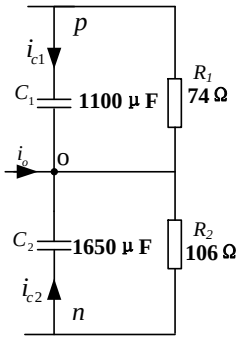

Fig.11 The DC-side equivalent circuit of asymmetric capacitor and unbalanced load

It is possible that capaci g-term fatigue, causing significant voltage offsets between the DC-link capacitors. To emulate this abnormal condition, two kinds of capacitors with different capacitance and manufacture are employed (C_1 is 1100μF with two CEB 2200μF/400V series, C_2 is 1650μF consists of two Jianghai company 3300μF/450V series). Similarly, two different resistors (R_1:74 Ω, R_2: 106 Ω) are used to emulate the unbalanced load, then the equivalent circuit is shown in Fig.11.

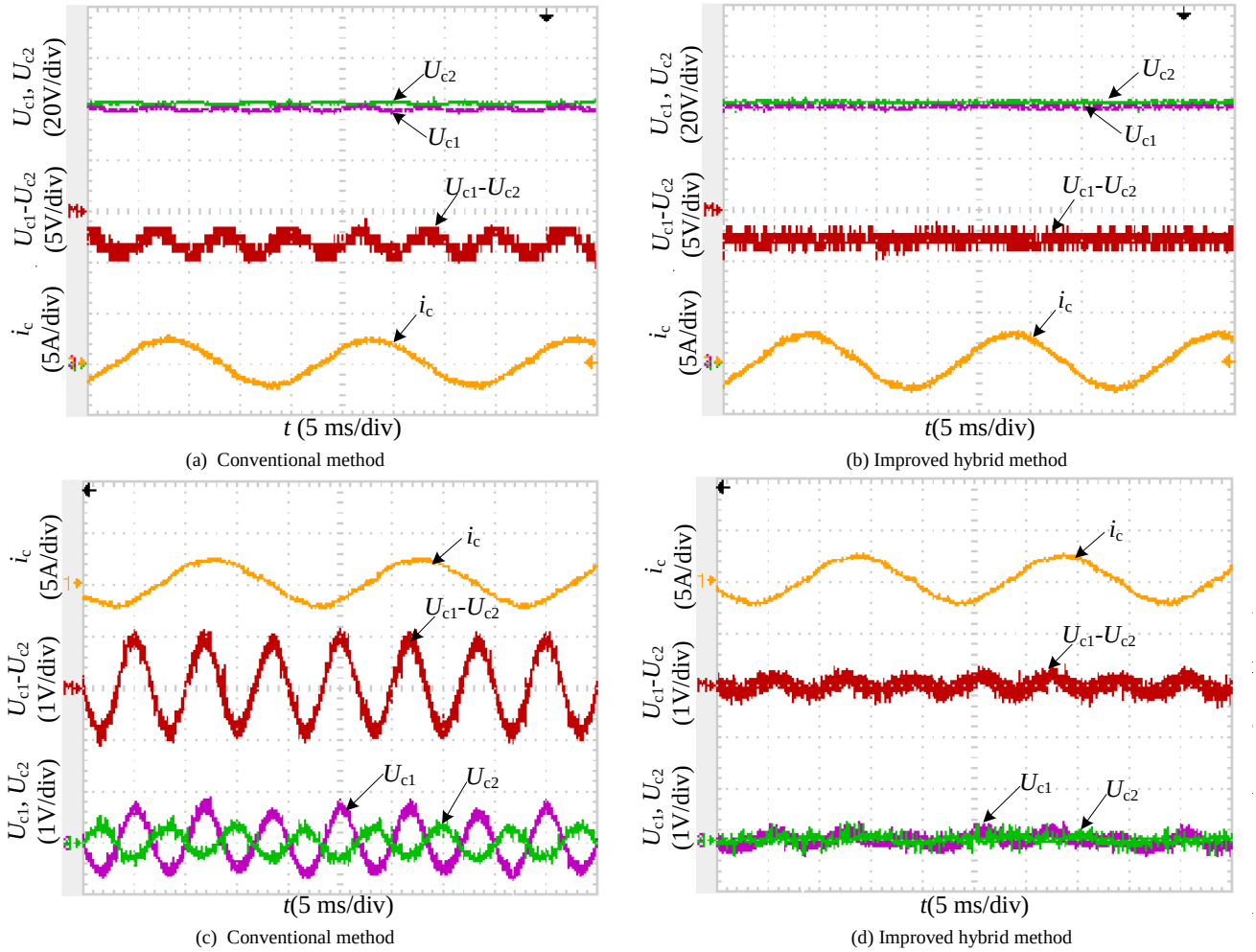

Fig. 12 The comparison waveforms between conventional fixed factor and improved hybrid algorithm ((c),(d): scope with AC channel)

fluctuation using AC coupling of the scope measurement channel as shown in Fig.12 (c), (d), it is also clear to see that the three times fundamental fluctuation can be effectively decreased using the improved hybrid method, which is a significant fluctuation when using conventional control methods.

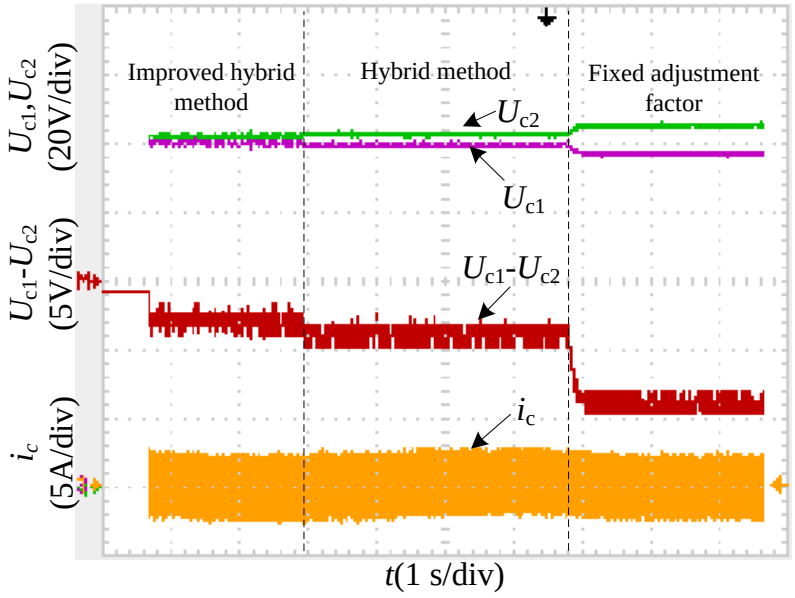

Fig.13 shows the influence

control methods. From the co

Fig.13 The influence comparison of neutral-point voltage deviation caused by asymmetric capacitor and unbalanced load with different cont

the conventional method of fixed adjustment factor, but by applying the hybrid method combining the dynamic adjustment factor and capacitor voltage deviation expression, the neutral-point voltage deviation is effectively reduced, however, the neutral-point voltage deviation is eliminated through using the improved hybrid method combining an additional adjustment coefficient.

Fig.14(a) and (b) show the input phase voltage， phase currents and output DC-link voltage. It can be seen that the input phase current is in phase with the input voltage resulting in a 0.99 input power factor obtained by experiment measurement. Moreover, the three-phase input currents are still sinusoidal and balanced under the proposed hybrid neutral-point control method.

Fig.15 shows the harmonic magnitude with and without proposed hybrid neutral point balancing control method, obtained using a power analyzer. Comparing the results it can be seen that the fundamental frequency current magnitude is increased as well as the current THD decreases from 4.21% to 3.8% using the proposed neutral point control method. Fig.16 shows a harmonic comparison using a relative value with and without proposed hybrid neutral point balancing control method. The low frequency harmonic caused by unbalanced capacitor voltage such as twice, third harmonics are greatly reduced, but the fourth, fifth, seventh, eleventh, thirteenth seventeenth harmonics are increased due to the deviation of the switching pulses. Fig.16 confirms that the proposed method effectively reduces low frequency input current harmonics, but at the expense of adding high-order harmonics, fortunately, these are easy to be filtered using a common filter.

Fig.17 (a), (b) shows the dynamic response waveforms of input phase current and output voltage when the steps from 70%load to 100%load and recovers to70%load. Seen from the waveform, the output voltage is maintained constant even though changes of the load. The constant DC component of output voltage is removed in order to observe this transient change using the AC coupled scope measurement channel shown in Fig.17 (b), it can be seen that output voltage recovers to steady state within 0.15s under the condition of transient adding 30%load, which shows the system with the proposed hybrid neutral-point control still exhibits a fast response to load disturbance.

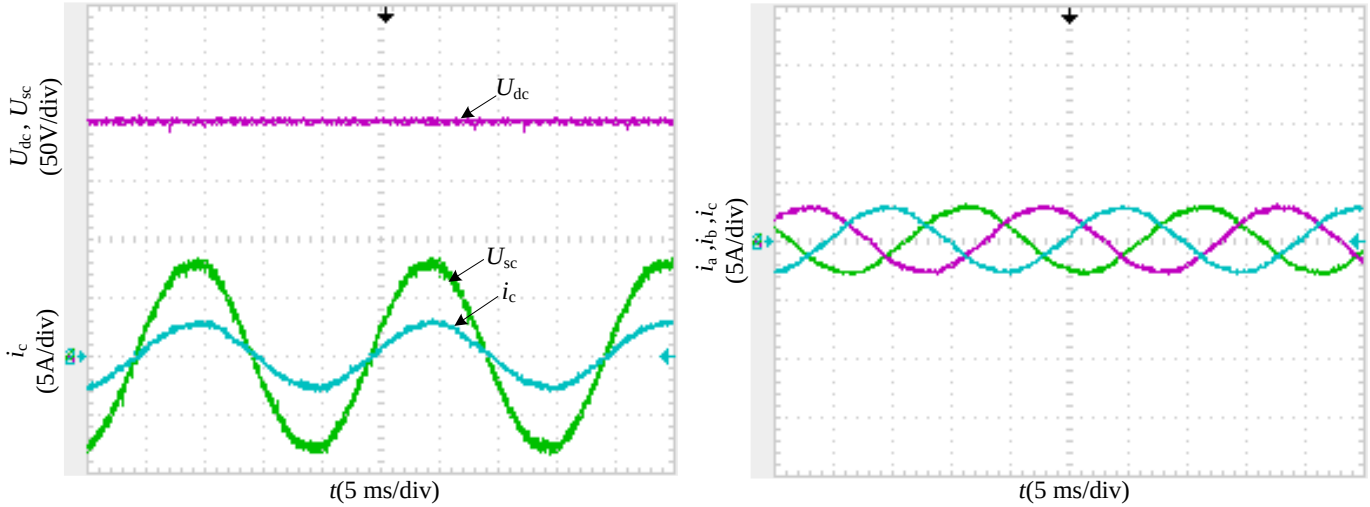

(a) Input phase voltage, current and output voltage (b) Three phase input currents

Fig. 14 The input voltage, current and output voltage waveforms under proposed hybrid neutral-point control method

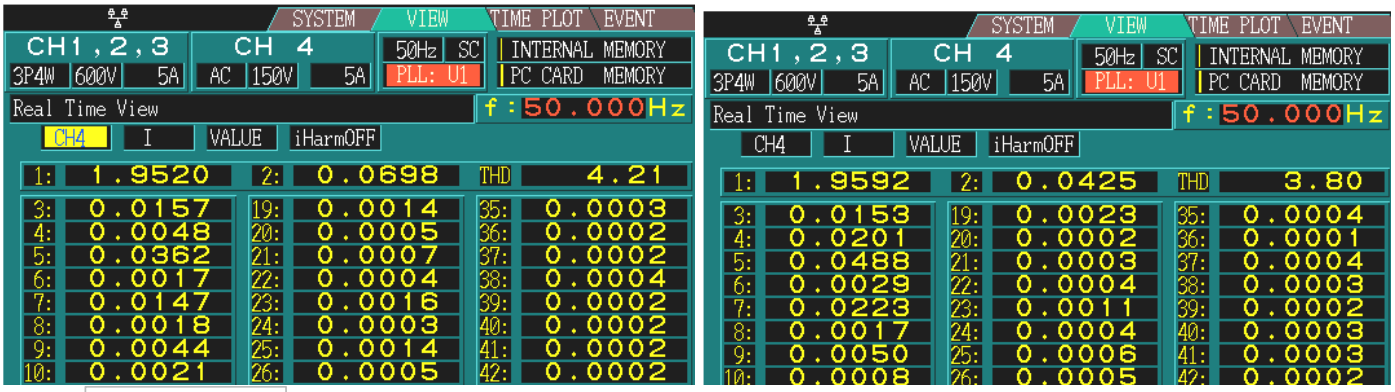

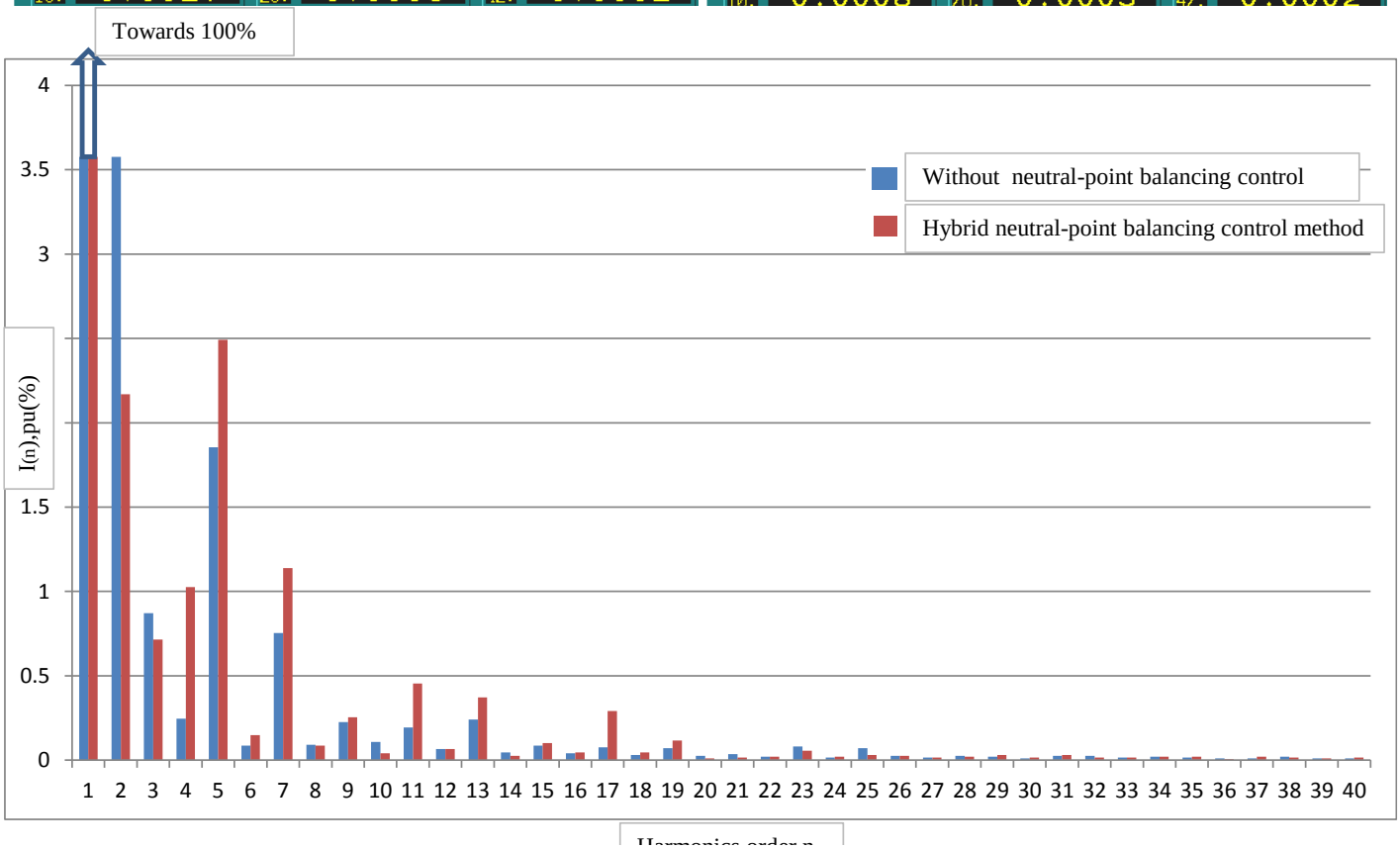

Fig

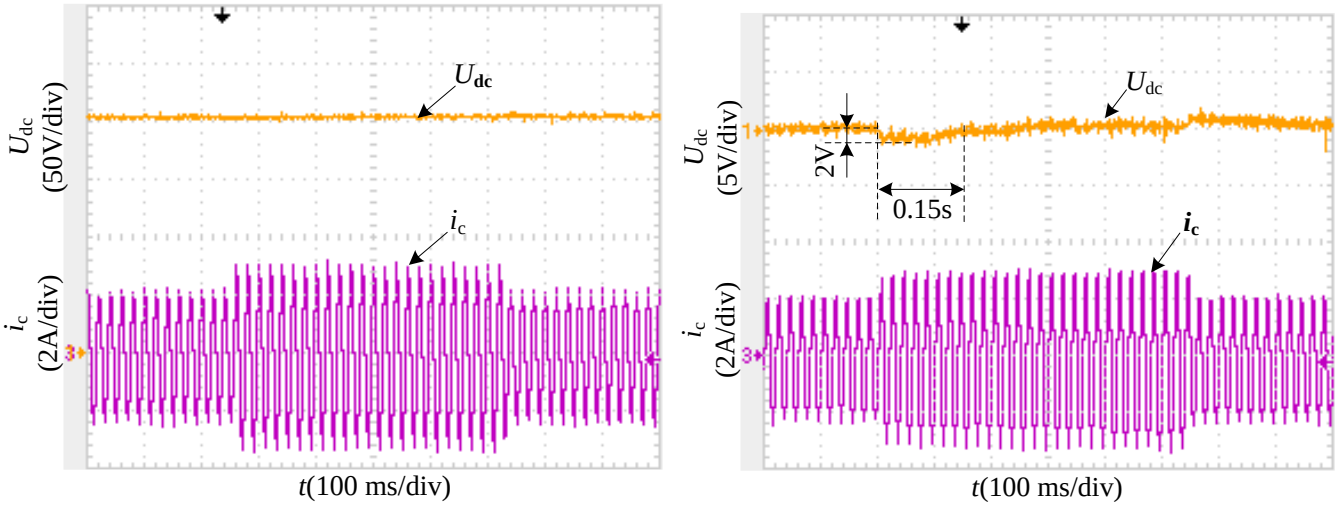

(a) Response when steps from 70%load to 100%load and recovers to 70%load (b) Special observing for dynamic response using scope coupling with AC channel

Fig. 17 The input and output waveforms under proposed hybrid neutral-point control method

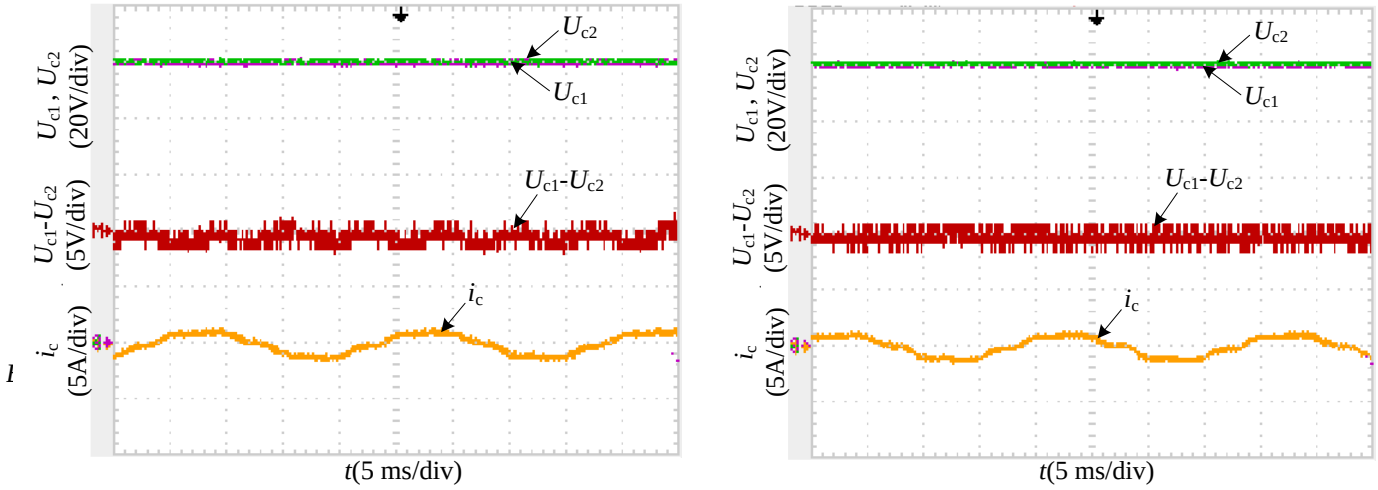

lig (a) Conventional method (b) Hybrid method

Fig.18 The comparison waveforms between conventional fixed factor and hybrid method under 100W output power

the three times fundamental frequency fluctuation component is effectively reduced using the proposed hybrid method even in a light load operating condition. But the input currents include more total harmonic distortion (THD) caused by working in the discontinuous conduction mode (DCM) in the light load condition [26]. This increased THD of input currents can be reduced using an enhanced control scheme as shown in [24]. Meanwhile, the VIENNA rectifier features an increased output voltage characteristic easily causing an overvoltage protection under the light load and especial for a no-load operating condition as mentioned in [28]. A specific circuit or control strategy should be used to make the system will work normally and remove the increased THD of input currents in these operating conditions, these are the author's future work.

V. Conclusion

This paper has presented a hybrid neutral-point balance control method combining a dynamic adjustment factor with a capacitor voltage deviation expression to solve the problem of neutral-point fluctuation in a VIENNA type three-level rectifier. Using a looking up table for capacitor voltage deviation and dynamic adjustment factor expression in the six input sectors, the neutral-point fluctuation can be effectively suppressed, so the influence of DC deviation in the DC-link capacitor voltage can be eliminated. Furthermore, significant fluctuation of neutral-point voltage caused by abnormal conditions such as asymmetric capacitor parameters or unbalanced loads can be reduced by employing the improved hybrid method, combining an additional adjustment coefficient. Moreover, the system after being introduced the proposed method still exhibits a low input current total harmonic distortion (THD), high displacement factor and fast response to load disturbance. In addition, the algorithm only needs a look up table, effectively removing the need for complex calculations which makes this method very suitable for practical implementation.

ACKNOWLEDGMENT

This work was supported by National Natural Science Foundation of China (51307138), Research Fund for the Doctoral Program of Higher Education of China (20126118120009), State Key Laboratory of Electrical Insulation and Power Equipment

(EIPE14207), doctor foundation of Xi'an University of technology (105-211104), special foundation of key disciplines of Shaanxi provincial project (105-5X1201)

REFERENCES

[1] Johann W.Kolar, Thomas.Friedli. "The essence of three-phase PFC rectifier systems-Part I ". *IEEE Trans.Power.Electron*, vol.28, no.1, pp.176-198,Jan.2013.

[2] Patrick.W.Wheeler, José Rodríguez, Jon C.Clare,Lee.Empringham,and Alejandro.Weinstein. "Matrix converters: A technology review". *IEEE Trans.Ind.Electron*, vol.49, no.2, pp.276-288,Apr.2002.

[3] Jacobus Daniel van Wyk and Fred C. Lee, "On a Future for Power Electronics", *IEEE J. Emerg. Sel. Topics Power Electron*, vol.1, no.2, pp. 59-72, June.2013.

[4] Weizhang Song, Yanru Zhong,Hao Zhang,Xiangdong Sun,Qi Zhang,Wei Wang, "A Study of Z-Source Dual-Bridge Matrix Converter Immune to Abnormal Input Voltage Disturbance and with High Voltage Transfer Ratio," *IEEE Trans. Ind. Inform*, vol. 9, no. 2, pp. 828–838, May. 2013.

[5] Thomas Friedli, Michael Hartmann, and Johann W. Kolar, "The essence of three-phase PFC rectifier systems—Part II," *IEEE Trans.Power.Electron*, vol. 29, no. 2, pp. 543–560, Feb. 2014.

[6] Johann W. Kolar and Franz C. Zach, "A novel three-phase utility interface minimizing line current harmonics of high-power telecommunications rectifier modules," *IEEE Trans. Ind. Electron*, vol. 44, no. 4, pp. 456–467,Aug. 1997.

[7] R.Ansari,M.R.Feyzi,K.Akbari Hamed.N.Sadati,Y.Yasaei,S.Ouni, "Input-Output linearization of a fourth-order input-affine system describing the evolution of a three-phase/switch/level(Vienna) rectifier," IET *Power. Electron*, vol. 4,Iss. 8, pp. 867–883, May. 2010.

[8] Lijun Hang, Ming Zhang, Leon M.Tolbert,Zhengyu Lu, "Digitized feedforward compensation method for high-power-density three-phase Vienna PFC converter," *IEEE Trans. Ind. Electron*, vol. 60, no. 4, pp. 1512–1519, April. 2013.

[9] June-Seok Lee and Kyo-Beum Lee. "Carrier-Based Discontinuous PWM Method for Vienna Rectifiers". *IEEE Trans.Power.Electron*, vol.30,no.6, pp.2896-2900,June.2015.

[10] Kolar W. Johann, Franz C. Zach. "A novel three-phase utility interface minimizing line current harmonics of high-power telecommunications rectifier modules," *Proc IEEE Int Commun Energy Conf*, Vancouver, BC, Canada,Nov,1994, pp.367-374.

[11] Lijun Hang, Hao Zhang, Sensen Liu.Xiaogao Xie,Chen Zhao,Shirong Liu, "A Novel Control Strategy Based on Natural Frame for Vienna-Type Rectifier Under Light Unbalanced-Grid Conditions," *IEEE Trans. Power. Electron*, vol. 62, no. 3, pp. 1353–1362, Mar. 2015.

[12] M. Hartmann, S. D. Round, H. Ertl, and J. W. Kolar, "Digital current controller for a 1 MHz, 10 kW three-phase VIENNA rectifier," IEEE Trans. Power Electron., vol. 24, no. 11, pp. 2496–2508, Nov. 2009.

[13] Rolando Burgos, Rixin Lai, Yunqing Pei, Fei(Fred) Wang,Dushan Boroyevich,Josep Pou." Space Vector Modulator for Vienna-Type Rectifiers Based on the Equivalence Between Two-and Three-Level Converters: A Carrier-Based Implementation". *IEEE Trans. Power. Electron*,Vol.23,no.4, pp.1888-1898,July,2008.

[14] J Alahuhtala, J Virtakoivu, T Viitanen,M.Routimo,H.Tuusa. "Space Vector Modulated and Vector Controlled Vienna I Rectifier with Active Filter Function," In *Proceeding of 4th IEEE International Conference on Power Conversion Conference*(PCC), Nagoya,Japan, April,2007,pp.62-68.

[15] Sergio Busquets Monge,Sergio Somavilla,Josep Bordonau,Dushan Boroyevich. "Capacitor Voltage Balance for the Neutral-point-clamped Converter using the Virtual Space Vector Concept with Optimized Spectral Performance,". *IEEE Trans. Power. Electron*, Vol.22,no.4, pp.1128-1135,July,2007.

[16] Ramkrishan Maheshwari,Stig Munk-Nielsen,Sergio Busquets-Monge. "Design of Neutral-point Voltage Controller of a Three-level NPC Inverter with Small DC-link Capacitors," *IEEE Trans. Ind. Electron*, Vol.20,no.5,pp.1861-1871,May,2013.

[17] Zhen Wang,Guojun Tan,Weijun Zen. "Research on VIENNA Rectifier Based on SVPWM," *Electric Drive*, Vol.41,no.4,pp.31-34,April,2011(in Chinese).

[18] Johann W.Kolar, Uwg Drofenik, F.C.Zach. "Current Handing Capability of the Neutral Point of a three-phase/Switch/Level Boost-Type PWM(VIENNA) Rectifier," *In Proceedings of 27th Annual IEEE Power Electronics Specialists Conference(PESC)*, Maggiore,Italy,June,1996,pp.1329-1336.

[19] Xinyu Wang,Yinjie He,Jinjun Liu. "Neutral-point Voltage Balancing Principle of NPC Inverter Modulated by SPWM Injected Zero-Sequence,"*Transactions of China Electrotechnical Society*,Vol.26,no.5,pp.70-77,May,2011.(in Chinese) .

[20] Ming Zhang, Lijun Hang,Wenxi Yao, Zhengyu Lu, Leon M.Tolbert. "A Novel Strategy for Three-phase/switch/level(Vienna) Rectifier under Severe Unbalanced Grids,". *IEEE Trans. Ind. Electron*.Vol.60,no.10,pp. 4243~4252,Oct,2013.

[21] Lijun Hang, Bin Li,Ming Zhang,Yong Wang, Leon M.Tolbert. "Equivalence of SVM and Carrier-based PWM in Three Phase Wire/Lever Vienna Rectifer and Capibility of Unbalanced Load Control,". *IEEE Trans. Ind. Electron*.Vol.61,no.1,pp. 20~28,Jan,2014.

[22] Weizhang Song,Jun Huang,Yanru Zhong. "Hysteresis Current Control Method of VIENNA Rectifier With Midpoint Potential Balance Control,".*Power System Technology*,Vol.37,no.7,pp.1909-1914,July,2013.(in Chinese).

[23] Ismael Araujo-Vargas, Andrew J. Forsyth, F. Javier Chivite-Zabalza. "Capacitor Voltage-Balancing Techniques for a Multipulse Rectifier With Active Injection,". *IEEE Trans. Ind. Appl*.Vol.47,no.1,pp. 185~198,January/February,2011.

[24] Mario Marchesoni,Paolo Segarich,Ernesto Soressi. "A New Control Strategy for Neutral-point-Clamped Active Rectifiers,". *IEEE Trans.Ind. Electron*,Vol.52,no.2,pp.462-470,April,2005.

[25] She Hongwu,Lin Hua,Wang Xingwei,Xiong Song,He Bi."Matrix Converter Control Strategy Under Abnormal Input Voltage," *Proceedings of the Chinese Society for Electrical Engineering*,vol.29,no. 33,pp.28-33,Nov,2009.(in Chinese).

[26] Peter Ide, Frank Schafmeister,Norbert Fröhleke, Horst Grotstollen. "Enhanced Control Scheme for Three-phase Three-level Rectifiers at Partial Load,". *IEEE Trans. Ind. Electron*.Vol.52,no.3,pp. 719~726,June,2005.

[27] Jian Sun,Daniel M. Mitchell, Matthew E Greuel, Philip T. Krein, Richard M. Bass. "Modeling of PWM Converters in Discontinuous Conduction Mode - A Reexamination," In Proceedings of 29th Annual IEEE Power Electronics Specialists Conference(PESC), Fukuoka,Japan,May,1998,pp.615-622.

[28] M.Makoschitz, M.Hartmann,H.Ertl. “Analysis of a Three-phase Flying Converter Cell Rectifier Operating in Light/No-load Condition,”. *The 30th Applied Power Electronics Conference and Exposition(APEC2015)* , North Carolina,USA,March,2015,pp. 92~100.